AIP Journal of Applied Physics

Thermal conductivity of self-assembled nano-structured ZnO bulk ceramics

Yu Zhao, Yongke Yan, Ashok Kumar, Hsin Wang, Wallace D. Porter, and Shashank Priya

Citation: Journal of Applied Physics **112**, 034313 (2012); doi: 10.1063/1.4745034
View online: http://dx.doi.org/10.1063/1.4745034
View Table of Contents: http://scitation.aip.org/content/aip/journal/jap/112/3?ver=pdfcov
Published by the AIP Publishing

Thermal conductivity of self-assembled nano-structured ZnO bulk ceramics

Yu Zhao,[1,a)] Yongke Yan,[1] Ashok Kumar,[1] Hsin Wang,[2] Wallace D. Porter,[2] and Shashank Priya[1,a)]
[1]*Bio-Inspired Materials and Devices Laboratory (BMDL), Center for Energy Harvesting Materials and Systems (CEHMS), Virginia Tech, Blacksburg, Virginia 24061, USA*
[2]*Materials Science and Technology Division, Oak Ridge National Laboratory, Oak Ridge, Tennessee 37831, USA*

(Received 23 May 2012; accepted 11 July 2012; published online 8 August 2012)

In this study, we describe the changes in thermal conductivity behavior of ZnO-Al micro- and nano-two-phase self-assembled composites with varying grain sizes. The reduction in thermal conductivity values of micro-composites was limited to ~15% for ZnO-4% Al. However, nano-composites exhibited large reduction, by a factor of about three, due to uniform distribution of nano-precipitates ($ZnAl_2O_4$) and large grain boundary area. Interestingly, the micro-composites revealed continuous decrease in thermal conductivity with increase in Al substitution while the nano-composites exhibited the lowest magnitudes for 2% Al concentration. Raman spectra indicated that phonon confinement in ZnO-Al nano-composites causes drastic decrease in the value of thermal conductivity. © *2012 American Institute of Physics*. [http://dx.doi.org/10.1063/1.4745034]

INTRODUCTION

Thermoelectric (TE) materials for application in waste heat recovery should be stable at elevated temperatures (>500 °C) and exhibit high figure of merit (zT) for high efficiency and reliability. The coefficient zT is defined as: $\alpha^2\sigma T/(\kappa = \kappa_{ph} + \kappa_{el})$, where α is the Seebeck coefficient, σ *is* the electrical conductivity, T is the absolute temperature, k is the thermal conductivity, κ_{ph} is the phonon contribution to κ, and κ_{el} is the electron contribution to κ. Semiconductors are usually considered as good thermoelectrics due to their large Seebeck coefficient and moderate carrier concentration[1] which leads to high power factor $\alpha^2\sigma$ and low κ values (much larger κ_{ph} compared to κ_{el}). Recently, interest has surged towards the investigation of semiconducting alloy based thermoelectric materials which have shown good power factor (10–100 μW cm^{-1} K^{-2}) and low κ values (around 1 Wm^{-1} K^{-1}) associated with controlled phonon scattering.[2] However, scarcity of elements in the optimized compositions, expensive synthesis techniques to achieve good density, and poor durability at elevated temperatures limit the potential of alloys. Some less toxic and abundantly available oxides have also been considered as the promising materials for thermoelectric devices such as Co-based p-type $NaCo_2O_4$ and $Ca_3Co_4O_{9+\delta}$ single crystals.[3,4] Modified $Ca_3Co_4O_{9+\delta}$ polycrystalline material has revealed zT of 0.61 at 1118 K.[5] We believe that these oxide based materials could provide cheaper and environmentally friendly alternative to the tellurides and other alloy compositions.

Doped ZnO is another promising n-type semiconductor due to its good Seebeck coefficient (around 200 μV/K) and substantial stability at elevated temperatures (up to 1000 °C).[6] The Zn-O bond has a covalent character because of small electronegativity difference which could lead to relatively large carrier mobility.[7] However, the simple wurtzite crystal structure and light Zn and O elements result in thermal conductivity as high as 100 W/m K at room temperature.[8] The reduction of κ becomes a primary and essential task towards improving the zT of ZnO. In the case of alloy TE materials, substantial progress has been realized in reduction of κ which could be attributed to strong phonon scattering by nanostructure.[2] Further, it has been reported that the lattice thermal conductivity (κ_{ph}) contributes 90% or more towards the overall thermal conductivity of ZnO.[7] Therefore, control of phonon propagation in crystal lattice becomes significant factor towards lowering the value of κ.

The centers for phonon scattering can be point defects, grain boundaries, nano-size inclusions, and pores.[8] Using combustible nano-sized polymer particles as a void forming agent (VFA), the nano-sized void introduced in ZnO matrix was shown to reduce κ values by 16%–25%.[9] However, milling with VFA may cause severe deterioration of electrical property. Foaming technique employing polystyrene to introduce micro-pores in ZnO has been used but it did not have significant effect on the value of κ.[10] The thermal conductivity of ZnO has been noticed to decrease with Al doping.[7,11,12] Co-doping with Ga in Al-doped ZnO showed reduction in the value of κ to ~5 W/mK.[13] The strong suppression in the value of κ was attributed to the granular texture due to Ga impurity; however, ZnO ceramics with large concentration of Ga were highly porous. Also, due to the limited solubility of Al in ZnO,[14] the secondary phase easily precipitates in ZnO matrix, which contributes toward κ reduction as well. Recently, nano inclusions have been used as phonon scattering centers in bulk ZnO samples and were found to reduce the thermal conductivity substantially (~15% of bulk value).[15] The reduction of κ was ascribed to ZnO nanograin, ZnO-$ZnAl_2O_4$ boundary, point defects, and

a)Authors to whom correspondence should be addressed. Electronic addresses: spriya@vt.edu and zhaoyu@vt.edu. Tel.: +1 540 231 0745. fax: +1 540 231 2903.

porosity (~90% relative density). It is still not clear that which of these factors play dominant role and how the substructure size modifies the thermal conductivity behavior. Thus, more systematic experiments are required to clarify the mechanism. In this paper, we address this subject by conducting systematic experiments on micro and nano self-assembled ZnO composites to understand the effect of precipitate size and grain size on κ.

EXPERIMENTAL

Two sets of $Zn_{1-x}Al_xO$ ($0 \leq x \leq 0.04$) samples were synthesized using solid-state reaction method. For first set of samples, micron-size precursor powders, ZnO (~75 μm, purity >99.9%, Alfa Aesar) and Al_2O_3 (~60 μm, purity >99.9%, Alfa Aesar) were used. These samples were sintered at 1400 °C for 5 h in air to obtain micron-size grains. The second set of samples was synthesized using nano-size precursor powders, ZnO (~30 nm, purity >99.7%, Advanced Materials LLC) and Al_2O_3 (40–50 nm, purity >99.5%, Alfa Aesar), and sintered at 1100 °C for 5 h in air to obtain ZnO with nano-size precipitated phase. Further, to study the influence of ZnO grain boundary area, pure ZnO samples were synthesized using ZnO (~30 nm, purity >99.7%, Advanced Materials LLC) powders. These samples were sintered subsequently by one-step sintering (1100 °C, 1000 °C, and 950 °C for 5 h) and two-step sintering (first heating up to 1000 °C holding for 1 min, cooling to 825 °C holding for 5 h with the rate of 4 °C per min and 20 °C per min, respectively) to achieve different grain sizes. The phase(s) and microstructure(s) of the samples were examined by using an X-ray diffractometer (XRD, PANalytical X'Pert, CuKa; Philips, Almelo, the Netherlands) and scanning electron microscopy (SEM, LEO (Zeiss) 1550 field-emission). The Oxford INCA Energy E2H X-ray energy dispersive spectrometer (EDS) system with silicon drifted detector was utilized for elemental mapping. The thermal conductivity was determined by combining thermal diffusivity measured using TA Instruments FL5000 flash diffusivity system and Cp measured using Netzsch 404 DSC. The Raman spectrum was collected using 100 mW–514 nm argon laser integrated with JY Horiba LabRam HR800 (high resolution 800 mm focal length spectrometer) and Andor electronically cooled CCD detection system (1024 × 256).

RESULTS AND DISCUSSION

X-ray diffraction (XRD) patterns of the sintered $Zn_{1-x}Al_xO$ pellets are shown in Figs. 1(a) and 1(b), respectively, revealing hexagonal wurtzite type zinc oxide phase formation (JCPDS # 36-1451). The samples synthesized using micron-size powders exhibited a and c lattice parameters as 3.245(9) and 5.201(4) Å ($x = 0.0$). Incorporation of Al in the ZnO lattice leads to shrinkage and subsequently lowering of a and c values to 3.243(0) and 5.199(3) Å, respectively, (Al content $x = 0.02$). It is evident that ionic radius of Al^{3+} (0.39 Å) in four-fold coordination is smaller than Zn^{2+} (0.60 Å) and therefore, if Al^{3+} occupies Zn^{2+} sites, a decrease in lattice parameter should be noticed.[16] An increase in Zn vacancies may also lead to the decrease in the value of lattice parameters a and c. XRD patterns of the samples obtained using nano-size precursor powders exhibited lattice parameters as $a = 3.247(5)$ and $c = 5.203(5)$ Å at "x" = 0. The nanostructured samples also showed slight decrease in lattice parameter with increasing Al content. Typical values of a and c being [3.248(9) Å, 3.247(5) Å, 3.246 (5) Å] and [5.202(0) Å, 5.201(2) Å, 5.200(2) Å] for Al content $x = 0.01$, 0.02, and 0.03, respectively. Further, on examining the XRD patterns carefully a signature of precipitated gahnite phase, $ZnAl_2O_4$, (JCPDS # 5–0669) can be noticed in all the $Zn_{1-x}Al_xO$ samples with Al content "x" > 0.01, which is marked with arrow in Fig. 1.

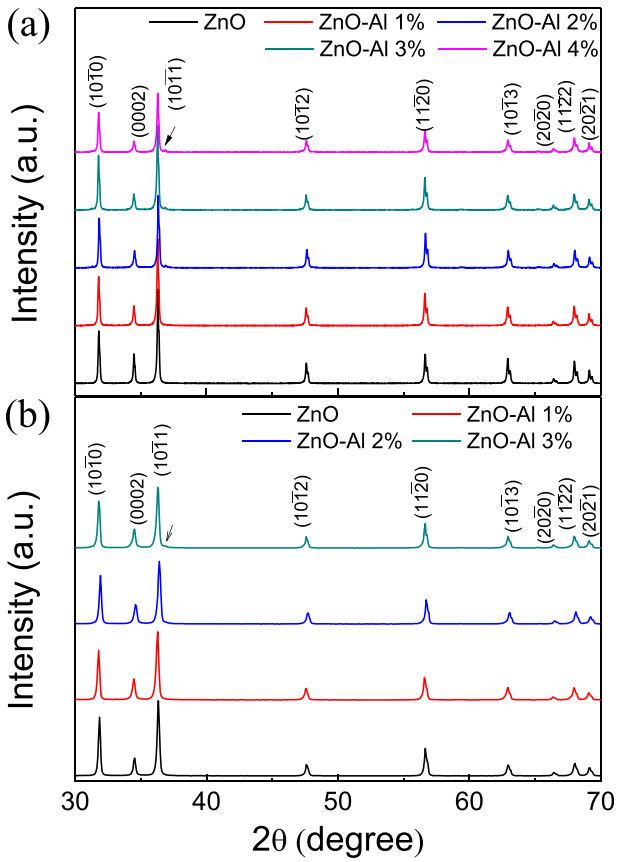

FIG. 1. XRD patterns of ZnO-Al (a) micro-composites; (b) nano-composites.

Figure 2 shows the scanning electron micrographs of two series of sintered $Zn_{1-x}Al_xO$ pellets. A small amount of $ZnAl_2O_4$ precipitates can be observed in all ZnO-Al samples. Increase in Al incorporation enhances the formation of gahnite precipitates and inhibits grain growth in both series of samples. Typical values of micron-size precipitates being 1–3 μm for the ZnO-4%Al samples synthesized using micron-size powders (ZnO-Al micro-composites). Elemental mapping performed using EDS on a typical $Zn_{0.96}Al_{0.04}O$ samples synthesized using micron-size precursor powder confirmed that $ZnAl_2O_4$ phase distributes uniformly and precipitates both inside and at grain boundaries of ZnO grains (Fig. 2(b)). The matrix grain size decreases with increase in Al content, but the change was not significant. The density estimated using Archimedes' method for ZnO-Al micro-composites containing 0%, 1%, 2%, 3%, and 4% Al was found to be more than 95%.

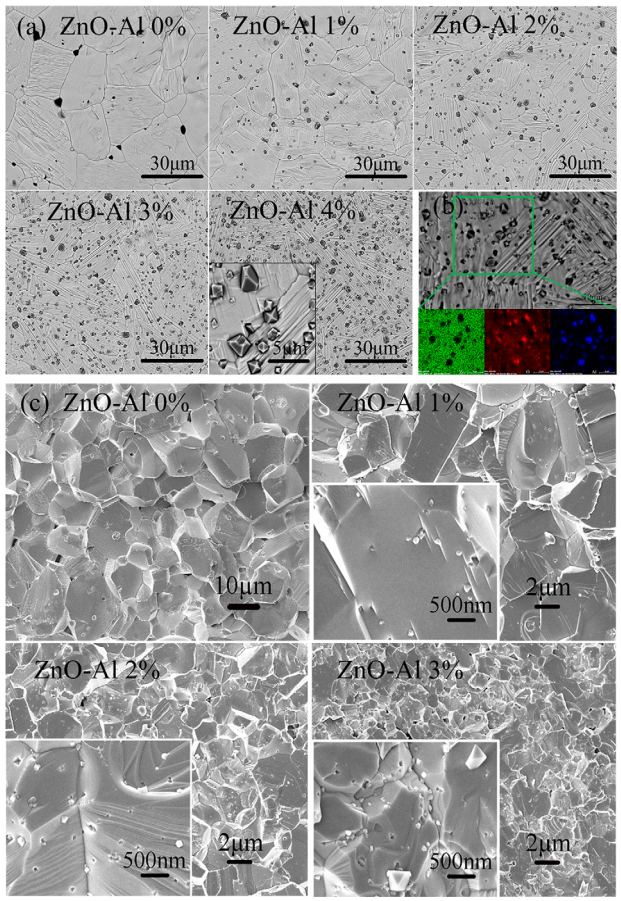

FIG. 2. (a) Contrast SEM images using backscattered electron of ZnO-Al micro-composites. The darker particles are $ZnAl_2O_4$ precipitates; (b) EDS elemental mapping of $(Zn_{0.96}Al_{0.04})O$ sample on element Zn, O, and Al; (c) SEM images of ZnO-Al nano-composites (cross section). The brighter particles are $ZnAl_2O_4$ nano precipitates and inserts are higher magnification SEM.

Figure 2(c) shows the scanning electron micrograph of the $Zn_{1-x}Al_xO$ $(0 \leq x \leq 0.03)$ samples synthesized using nano-size precursor powders. The grain size is much smaller in comparison to the ZnO-Al micro-composites samples. Further, the grain size is drastically reduced with Al incorporation which indicates that the grain boundary pinning due to Al addition is more effective in the samples synthesized using nano precursor powders than that in the samples synthesized using micron-size precursor powders. The typical values of grain sizes for the ZnO-Al samples synthesized using nano-size precursor powders range from 1 to 5 μm for ZnO grains and 50–400 nm for $ZnAl_2O_4$ precipitates (ZnO-Al nano-composites). The density estimated using Archimedes' method for ZnO-Al nano-composites containing 0%, 1%, 2%, and 3% Al was found to be ~95% of relative density.

The thermal conductivity (κ) and thermal diffusivity (α) of both series of samples are shown in Fig. 3. The thermal conductivity was calculated from the following relation:

$$k = \rho \, \alpha \, C_p \qquad (1)$$

where C_p denotes the heat capacity. Both series of samples exhibited reduction in the values of κ with increasing temperature due to thermal softening and higher frequency phonon interactions at elevated temperatures.[17] However, with increasing Al content, micro- and nano-composites displayed different κ behavior. ZnO-Al micro-composites exhibited progressive decrease in the values of κ with increase in Al content; relative decrease in value of κ being ~15% for the samples containing 4% Al than those containing 1% Al at all temperatures. For ZnO-Al nano-composites, the reduction was much more obvious, especially in low temperature range. The value of κ drops to its minimum for the samples containing 2% Al and then increases again for 3% Al addition. The thermal conductivity of ZnO-2%Al was 7.5 W/m K at room temperature and then decreases to 3.7 W/m K at 600 °C. These values are 73% and 40% lower than pure ZnO samples synthesized under the same conditions. Since more than 90% of thermal conductivity is associated with κ_{ph}, the major contribution should mainly come from phonon scattering. It is well-known that the contribution of phonon-phonon and phonon-electron scatterings is low below the Debye temperature (~400 K for ZnO).[8] The phonon-boundary and phonon impurity scatterings play dominant role at relative low temperature to achieve low κ. According to the observations from SEM and XRD, both series of ZnO-Al composites possess two main differences from pure ZnO: namely presence of self-assembled precipitates and grain size, (due to comparable and high densities, both group of samples have been assumed to reveal similar porosity effect on phonon scattering). Both the disordered $ZnAl_2O_4$/ZnO and ZnO/ZnO boundaries will act as the potential sites for phonon scattering. Moreover, the scale of precipitates and grain size of ZnO-Al nano-composites were much smaller than those of ZnO-Al micro-composites. For understanding the mechanism of phonon scattering in nano-composites, Raman spectroscopy was utilized.

The vibrational properties of the nano-composite ZnO-Al samples investigated using laser Raman spectra are shown in Fig. 4. The wurtzite ZnO belongs to the C_{6v}^4 space group with four atoms per unit cell and from the 12 possible vibrational modes only the A_1, E_1, and E_2 are Raman-active optical modes.[8] Further, due to ionic character of Zn–O bonds, polar modes (A_1 and E_1) exhibit large splitting as longitudinal optical (LO) and transverse optical (TO) modes. The appearance of a high intensity, sharp and strong peak around 440 cm^{-1} is attributed to the Raman active optical phonon E_2 mode of the ZnO. It is obvious that the mode "E_1-high" is much stronger in the ZnO-Al samples in comparison to pure ZnO samples. Theoretical reports on phonon confinement in ZnO nanostructure have predicted confined LO phonon wavenumber to be between A_1 (LO) (574 cm^{-1}) and E_1 (LO) (590 cm^{-1}).[17] Experimental studies have found confined LO phonon modes to appear at 588 cm^{-1} (for 8.5 nm) and 584 cm^{-1} (for 4.0 nm).[19,20] We believe the higher intensity at 584.5 cm^{-1} is attributed to nano-size precipitated phase in ZnO-Al nano-composites. No significant peak shift was noticed for any of the phonon modes (inset Fig. 4). It has been reported that peak shift and broadening of the Raman peaks are observed when quantum dot size approaches to exciton Bohr radius.[18,21] It is believed that the size of the nano-precipitated phase in ZnO-Al nano-

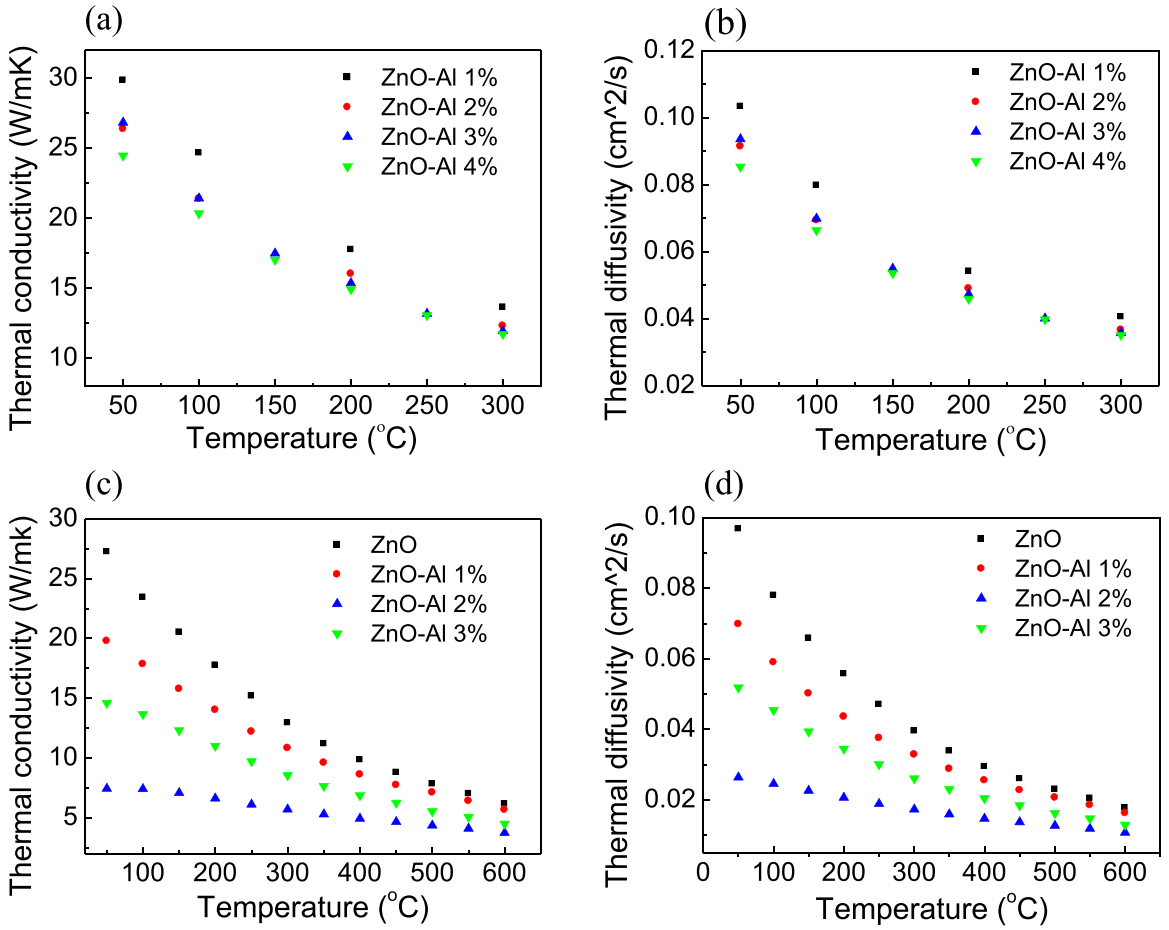

FIG. 3. Temperature dependence of thermal diffusivities and thermal conductivities of ZnO-Al (a) and (b) micro-composites; (c) and (d) nano-composites.

composites is effective for phonon confinement but not small enough to exhibit peak shift and broadening. Therefore, phonon scattering at ZnO/$ZnAl_2O_4$ boundary occurred in both ZnO-Al micro- and nano-composites, and phonon confinement in the homogeneously distributed nano-precipitates leads to larger decrease in the value of κ.

Furthermore, κ reduction of ZnO-Al nano-composites varies with the amount of Al. κ drops significantly from pure ZnO to ZnO containing 2% Al and then increases again for 3% Al addition, which indicates the difference of phonon relaxation time. The phonon scattering behavior generally depends on four mechanisms: Umklapp phonon-phonon scattering, phonon-impurity scattering, phonon-boundary scattering, and phonon-electron scattering. So the combined relaxation time can be given as[22]

$$\frac{1}{\tau_C} = \frac{1}{\tau_U} + \frac{1}{\tau_M} + \frac{1}{\tau_B} + \frac{1}{\tau_{ph-e}}, \tag{2}$$

where τ_C, τ_U, τ_M, τ_B, and $\tau_{ph\text{-}e}$ denote total, Umklapp phonon-phonon scattering, phonon-impurity scattering, phonon-boundary scattering, and phonon-electron scattering relaxation times, respectively. Assuming additional Al^{3+} ions stay in precipitates, the Umklapp phonon-phonon scattering, phonon-impurity scattering, and phonon-electron scattering in ZnO-Al nano-composites can be considered to be comparable, so cannot lead to large κ difference. Because of the formation of nano-precipitates and grain size reduction, phonon-boundary scattering is the key factor for κ variation which can be expressed as[22]

$$\frac{1}{\tau_B} = \frac{V}{D}(1-p), \tag{3}$$

where V is the phonon group velocity, D is the dimension of the system, and p is the surface roughness. The value of p

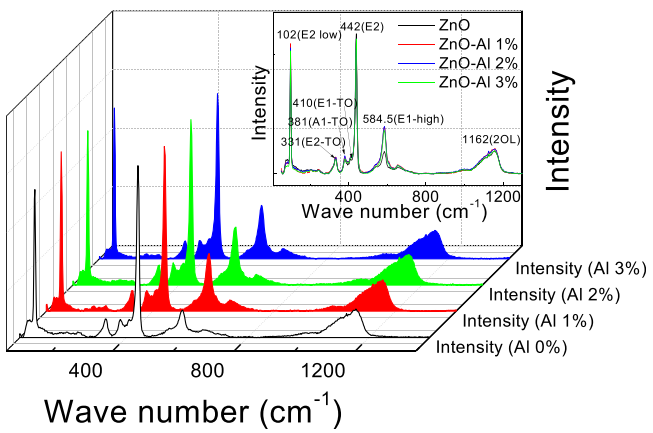

FIG. 4. Raman spectra of ZnO-Al nano-composites.

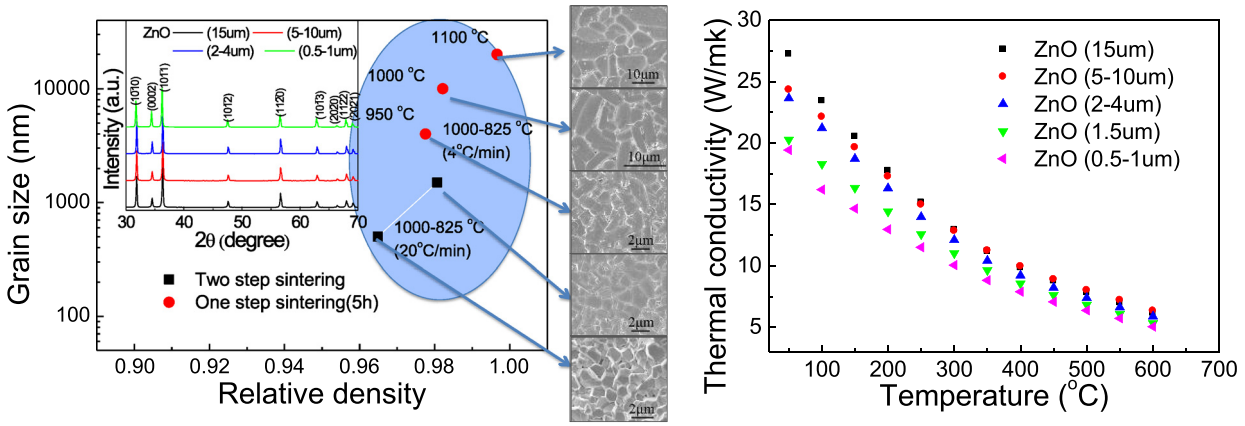

FIG. 5. Grain size vs. relative density, SEM images and temperature dependence of thermal conductivity of ZnO with different grain size, inset is XRD patterns.

close to 1 means a smooth surface where the scattering is purely specular and the relaxation time goes to ∞; hence, boundary scattering does not affect thermal transport. Due to the different lattice arrangement at ZnO/$ZnAl_2O_4$ boundary this is a possibility. With increase of Al additive to 2%, the precipitate increases resulting in reduction of κ especially at low temperature range. When Al concentration increases to 3%, the size of precipitates increases to 300–400 nm, resulting an increase in magnitude of κ.

ZnO/ZnO grain boundary is another phonon-boundary scattering center since ZnO grains shrink from $\sim$10 μm for pure ZnO to less than 2 μm for ZnO-Al nano-composites (x = 0.03). Accordingly, ZnO samples with various grain sizes were synthesized to clarify the contribution arising from ZnO/ZnO grain boundary area. The value of grain sizes varied from 0.5–1 μm to 10–15 μm depending on whether one-step sintering or two-step sintering at different heating rate was used for synthesis (Fig. 5). All the sintered samples exhibited pure hexagonal wurtzite structure with relative density higher than 96%. It can be noticed in the figure that κ reduction with smaller grain size is more evident at lower temperatures (<200 °C). Its values at room temperature for ZnO samples with grain sizes of 5–10 μm, 2–4 μm, 1.5–2 μm, and 0.5–1 μm compared to the large grain size (10–15 μm) are reduced by 10%, 13%, 25%, and 28%, respectively. At elevated temperatures, ZnO with grain sizes 10–15 μm, 5–10 μm, and 2–4 μm has almost the same κ (the difference is less than 5%). However, smaller grains, such as 1.5–2 μm and 0.5–1 μm revealed reduction in the value of κ by $\sim$13% and 18%, respectively. These findings confirm that grain boundary area also has significant contribution towards the reduction in thermal conductivity but smaller than the contribution due to nano-precipitates.

CONCLUSIONS

In summary, Al-modified ZnO samples were synthesized using micron- and nano-size precursor powders through solid state reaction. Incorporation of aluminum in ZnO resulted in the precipitation of gahnite $ZnAl_2O_4$, precipitates, which, in turn, inhibited grain growth. At 2 at. % Al content, $ZnAl_2O_4$ precipitates in ZnO-Al nano-composites exhibited 3-fold reduction in the values of thermal conductivity (κ). The reduction in the value of thermal conductivity for micro-composites was limited ($\sim$15% for ZnO-4% Al). The large κ reduction of ZnO-Al nano-composites was mainly attributed to phonon confinement by nano-size precipitates. The investigations on pure ZnO with varying grain sizes ($\sim$0.5–15 μm) revealed that ZnO/ZnO grain boundary area also has significant contribution towards the thermal conductivity.

ACKNOWLEDGMENTS

Authors gratefully acknowledge the financial support provided by NSF/DOE Thermoelectrics Partnership. The work was also supported by the Assistant Secretary for Energy Efficiency and Renewable Energy, Office of Vehicle Technologies as part of the High Temperature Materials Laboratory User Program at Oak Ridge National Laboratory managed by the UT-Battelle LLC, for the Department of Energy under Contract DEAC05000OR22725. One of Authors Yu Zhao would like to thank Charles Farley for his help with Raman spectra measurement.

[1]D. M. Rowe, *Thermoelectrical Handbook Macro to Nano* (CRC, 2006), pp. 1–8.
[2]J. R. Sootsman, D. Y. Chung, and M. G. Kanatzidis, Angew. Chem., Int. Ed. **48**, 8616 (2009).
[3]I. Terasaki, Y. Sasago, and K. Uchinokura, Phys. Rev. B **56**, R12685 (1997).
[4]M. Shikano and R. Funahashi, Appl. Phys. Lett. **82**, 1851 (2003).
[5]N. V. Nong, N. Pryda, S. Linderoth, and M. Ohtaki, Adv. Mater. **23**, 2484 (2011).
[6]M. Ohtaki, T. Tsubota, K. Eguchi, and H. Arai, J. Appl. Phys. **79**, 1816 (1996).
[7]T. Tsubota, M. Ohtaki, K. Eguchi, and H. Arai, J. Mater. Chem. **7**, 85 (1997).
[8]Ü. Özgür, Y. I. Alivov, C. Liu, A. Teke, M. A. Reshchikov, S. Doğan, V. Avrutin, S.-J. Cho, and H. Morkoç, J. Appl. Phys. **98**, 041301 (2005).
[9]M. Ohtakil and R. Hayashi, "Enhanced thermoelectric performance of nanostructured zno: a possibility of selective phonon scattering and carrier energy filtering by nanovoid structure," in *25th International Conference on Thermoelectrics, Vienna, Austria*, 6-10 August 2006, pp. 276–279.
[10]T. Teranishi, Y. Mori, H. Hayashi, and A. Kishimoto, J. Am. Ceram. Soc. **95**, 690 (2012).
[11]K. F. Cai, E. Müller, C. Drašar, and A. Mrotzek, Mater. Sci. Eng. B **104**, 45 (2003).
[12]K. H. Kim, S. H. Shim, K. B. Shim, K. Niihara, and J. Hojo, J. Am. Ceram. Soc. **88**, 628 (2005).

[13]M. Ohtaki, K. Araki, and K. Yamamoto, J. Electron. Mater. **38**, 1234 (2009).
[14]K. Shirouzu, T. Ohkusa, M. Hotta, N. Enomoto, and J. Hojo, J. Ceram. Soc. Jpn. **115**, 254 (2007).
[15]P. Jood, R. J. Mehta, Y. L. Zhang, G. Peleckis, X. L. Wang, R. W. Siegel, T. B.-Tasciuc, S. X. Dou, and G. Ramanath, Nano Lett. **11**, 4337 (2011).
[16]Z. B. Zhan, J. Y. Zhang, Q. H. Zheng, D. M. Pan, J. Huang, F. Huang, and Z. Lin, Cryst. Growth Des. **11**, 21 (2011).
[17]A. J. Kulkarni and M. Zhou, Appl. Phys. Lett. **88**, 141921 (2006).
[18]V. A. Fonoberov and A. A. Balandin, Phys. Rev. B **70**, 233205 (2004).
[19]M. Rajalakshmi, A. K. Arora, B. S. Bendre, and S. Mahamuni, J. Appl. Phys. **87**, 2445 (2000).
[20]V. A. Fonoberov and A. A. Balandin, Phys. Status Solidi C **1**, 2650 (2004).
[21]K. A. Alim, V. A. Fonoberov, and A. A. Balandin, Appl. Phys. Lett. **86**, 053103 (2005).
[22]J. Zou and A. Balandin, J. Appl. Phys. **89**, 2932 (2001).